scientific reports

OPEN

$CdS/CeO_2/Ag_2CO_3$ nanocomposite as an efficient heterogeneous catalyst for Knoevenagel condensation and acetylation reactions

Getachew A. Seid[1,2], Abi M. Taddesse[2], Neelaiah Babu[2] & Jemal M. Yassin[3]✉

Knoevenagel condensation and acetylation reactions play a critical role in organic synthesis by facilitating the formation of carbon-carbon bonds and the modification of functional groups; however, limitations like low efficiency and demanding reaction conditions and time underscore the necessity for developing better techniques to enhance their practical applications. In this study, a ternary nanocomposite of $CdS/CeO_2/Ag_2CO_3$ was synthesized by varying the molar ratio of CdS to CeO_2/Ag_2CO_3 using the precipitation method. This heterogeneous catalyst was developed for Knoevenagel condensation and acetylation reactions applications. The optical properties, functional groups, crystalline structure, morphology, and surface area of the synthesized catalysts were characterized using UV-Vis-DRS, FTIR, XRD, SEM, and N_2 adsorption-desorption isotherms, respectively. For the Knoevenagel condensation reaction between benzaldehyde and malononitrile, the optimal conditions were found to be the use of water as a solvent, at 10% w/w catalyst loading based on the total reagent mass, and room temperature (20 °C). Under these conditions, $CdS/CeO_2/Ag_2CO_3$ with a CdS: CeO_2/Ag_2CO_3 weight ratio of 3:1 gave high yields, 92.19 ± 0.41 in 33 min for Knoevenagel condensation and 93.8 ± 1.19 in just 3 min for the acetylation reaction. The reaction conditions were tested for different aromatic aldehydes with malononitrile, yielding high isolated products. The reusability of the $CdS/CeO_2/Ag_2CO_3$ (3:1) catalyst was assessed, with only a 6.4% decrease in yield after sixth consecutive runs under optimal reaction conditions. Furthermore, the optimized catalyst, $CdS/CeO_2/Ag_2CO_3$ (3:1), was evaluated for its catalytic activity in the acetylation of an aniline derivative. The structures of the synthesized products, 2-benzalidinemalononitrile and acetanilide, were confirmed by spectrometric techniques such as ^{1}H-NMR, ^{13}C-NMR, and FTIR analysis.

Keywords Knoevenagel condensation, Acetylation reaction, Ternary nanocomposite, 2-Benzalidinemalononitrile, Catalysis

Researchers are actively working to develop efficient heterogeneous catalysts for the Knoevenagel condensation and acetylation reactions. Knoevenagel condensation is a nucleophilic addition reaction that involves the reaction of an aldehyde with an active methylene compound, resulting in the formation of a new carbon-carbon double bond, yielding α,β-unsaturated carbonyl compounds crucial for pharmaceuticals and agrochemicals. Acetylation reactions modify functional groups, protect reactive sites, and are key in synthesizing drugs like aspirin[1]. The products of this reaction (2-Benzylidenemalononitrile and acetanilide) are used in the synthesis of heterocyclic compounds, medicinal intermediates, fine chemicals, drugs, natural products, fluorescent dyes, and functional polymers[2–5]. In the case of the acetylation reaction, a functional group, such as alcohols, amines, phenols, or thiols, undergoes acylation through a multi-step process that is key in drug synthesis[5,6]. This acylation is typically carried out using an acylating agent, such as acid chlorides or anhydrides, in the presence of either acidic or basic catalysts.

[1]Department of Chemistry, Dire Dawa University, P.O. Box 1362, Dire Dawa, Ethiopia. [2]Department of Chemistry, Haramaya University, P.O. Box 138, Dire Dawa, Ethiopia. [3]Department of Chemistry, Debre Berhan University, P.O. Box 445, Debre Berhan, Ethiopia. ✉email: jemalchemistry@gmail.com; jemalmohammed@dbu.edu.et

Conventionally, both the Knoevenagel condensation and acetylation reactions have relied on homogeneous catalysts, including basic catalysts such as 4-dialkylaminopyridines[6,7], ionic liquids[8], and pyridine[9], as well as acidic catalysts like Lewis acids. Notable examples of the latter include $Ce(OTf)_3$[10], $HClO_4$-SiO_2[11], $Gd(OTf)_3$[12], and 4-(N, N-dimethylamino) pyridine[13], which have been reported for acetylation reactions. For Knoevenagel condensation, weak organic bases such as urea[14], alkali metal hydroxides[15], and Lewis acids like CdI_2 and $BiCl_3$ have also been employed[16]. While these homogeneous catalysts show potential, they are often associated with significant drawbacks. Key issues include challenges in post-reaction separation and negative environmental impacts[17,18]. Additionally, these catalysts are non-recoverable and non-reusable, raising concerns regarding environmental safety.

Given the growing need for environmentally friendly, cost-effective, and energy-efficient methods for acetylation and Knoevenagel condensation, there is an urgent demand for simpler and more practical synthetic procedures. The use of heterogeneous catalysts offers a promising solution, addressing these challenges (like low catalytic efficiency, poor stability, and limited reusability) and providing a more sustainable approach[19–22]. Nanocatalysts, in particular, have emerged as a vital component of sustainable technology, especially in the fields of Knoevenagel condensation and acetylation reactions. These catalysts have garnered significant attention due to their non-corrosive nature, reusability, ability to produce pure products, and overall environmental friendliness when used under mild conditions[18,21,23,24]. Nanocatalysts are characterized by their unique properties, including a high surface area-to-volume ratio, small size, distinct electronic structure, and controlled particle arrangement and distribution, which contribute to their high thermal and chemical stability[25]. In heterogeneous catalysis, various types of nanocatalysts have been explored, including nano-supported catalysts[26], nano mixed metal oxides[27], and magnetic nanocatalysts[28]. Metal oxide catalysts, in particular, exhibit surface polarizing properties and facilitate electron transport, making them ideal for acid-base and redox catalytic reactions.

Metal oxides such as CeO_2[29], ZnO[30], magnetic silica-supported Ag_2CO_3[31], (CeO_2/ZrO_2)[32], and Ag@TiO_2[33] have been utilized in various organic reactions. However, these single and binary nanocatalysts often exhibit limited catalytic activity, poor durability, and low thermal stability.

To address these limitations, we aimed to improve the stability and catalytic performance of these materials by combining two or more carbonate and oxide semiconductors. Unlike previously reported nanocatalytic systems, we hypothesize that the ternary nanocomposite developed in this study will exhibit significantly enhanced catalytic activity for both the Knoevenagel condensation and acetylation reactions.

Building on our current protocol, we have developed a new Lewis acid-base heterogeneous CdS/CeO_2/Ag_2CO_3 nanocatalyst, utilizing water as a solvent for the Knoevenagel condensation and a solvent-free approach for the acetylation of aniline. To enhance catalytic performance, various preparation methods were explored, including sol-gel, co-precipitation, and high-temperature combustion techniques. Recently, CeO_2 nanoparticles synthesized through the pyrolysis of cerium metal-organic frameworks (Ce-MOFs) have demonstrated superior physicochemical properties, such as increased crystallinity, finer structure, and a higher concentration of oxygen vacancies and acidic sites on the surface, which are believed to boost catalytic efficiency[34]. The CeO_2 nanoparticles were successfully prepared by pyrolyzing Ce-MOFs at 500 °C and then combined with CdS and Ag_2CO_3 via co-precipitation method, resulting in a stable and highly efficient CdS/CeO_2/Ag_2CO_3 nanocatalyst. In this study, we report the use of CdS/CeO_2/Ag_2CO_3 based heterogeneous nanocatalyst for Knoevenagel condensation in water and solvent-free acetylation of aniline, providing easier work-up procedures and yielding products with better purity.

Experimental section

Materials

All chemicals and reagents were analytical grade and used as obtained without further purification. Cerium nitrate hexhydrated ($Ce(NO_3)_3$. $6H_2O$, 99.5%, Alfa Aesar), Terephtalic acid (H_2BDC, 98%, Acros Organic), Cadmium Acetate dihydrated ($Cd(CH_3COO)_2.2H_2O$, 98%, BDH,), Silver nitrate ($AgNO_3$, 99.8%, UNichem AR), Acetic anhydride $(CH_3CO)_2O$, 97%, Carloerba reagent), 4-Nitroaniline ($C_6H_6N_2O_2$, 98.5%, Blulux laboratory), Malononitrile ($CH_2(CN)_2$), 99%, Brtain), and Benzaldehyde (C_6H_5CHO, 99.5%, BDH).

Synthesis of catalyst

Preparation of CeO_2, Ag_2CO_3 and CdS nanoparticles

Before preparing CeO_2, cerium-based metal-organic frameworks (Ce(III)-BDC MOF) were first synthesized using a modified precipitation method at room temperature and water as the solvent, following a procedure adapted from previously reported methods[35]. In a separate beaker, 15 mmol (2.492 g) of H_2BDC (the linker) was dissolved in 70 mL of deionized water, while 10 mmol (4.342 g) of $Ce(NO_3)_3$•$6H_2O$ was dissolved in 30 mL of deionized water. The pH of the linker solution was adjusted to 7 using ammonia solution (V/V NH_3:H_2O, 1:1 ratio). The cerium solution was then added dropwise to the linker solution under continuous stirring for 1 h. A white precipitate formed which was collected by centrifugation at 2500 rpm for 20 min, washed three times each with deionized water and ethanol, and then dried at 60 °C for 24 h. The resulting product, Ce(III)-BDC MOF was calcined at 500 °C for 2 h in a furnace with a heating rate of 2 °C/min, yielding MOF-derived CeO_2 nanoparticles after cooling to room temperature.

Ag_2CO_3 nanoparticles were synthesized using the co-precipitation method, with modifications based on a prior report[36]. Initially, 30 mL of a 2.5 mmol (0.210 g) $NaHCO_3$ solution and 20 mL of a 5 mmol (0.849 g) $AgNO_3$ solution were prepared separately. The sodium bicarbonate solution was then added dropwise to the silver nitrate solution while stirring continuously for 1 h. The resulting precipitate was collected by centrifugation, washed three times with ethyl alcohol and distilled water, and then dried at 60 °C for 6 h.

CdS nanoparticle was conducted using the co-precipitation method with some modification[37]. Initially, equimolar (0.1 M) solutions of $Cd(CH_3COO)_2$·$4H_2O$ and Na_2S·$9H_2O$ were prepared separately. The Na_2S·$9H_2O$

solution was then added dropwise to the $Cd(CH_3COO)_2{\cdot}4H_2O$ solution while stirring continuously for 2 h. After the reaction, a yellow precipitate was collected by centrifugation and washed several times with distilled water and ethyl alcohol. The product was dried at 70 °C for 5 h and then calcined at 300 °C for 2 h.

Preparation of Ag_2CO_3/CeO_2 and CdS/CeO_2 composites

Ag_2CO_3/CeO_2 composite material was prepared using a simple chemical precipitation method with minor modification as previously reported[38]. Initially, 0.200 g of CeO_2 was dispersed in 60 mL of deionized water using an ultrasonic cleaner until a homogeneous solution was formed. Then, 6 mL of a 0.1 M aqueous solution of $AgNO_3$ was added dropwise to the dispersed solution, and the mixture was stirred for 30 min. Next, 6 mL of a 0.1 M aqueous solution of $NaHCO_3$ was added, and the solution was stirred for an additional 1.5 h using a magnetic stirrer to form the precipitate. The product was filtered, washed three times with ethanol and deionized water, and then dried at 60 °C for 12 h.

The preparation of CdS/CeO_2 binary composite was made following precipitation method[39]. Initially, 1.720 g of prepared CeO_2 was dispersed in 100 mL of distilled water using an ultrasonic cleaner for 30 min. Separately, 2.664 g of $Cd(CH_3COO)_2{\cdot}2H_2O$ was dissolved in 100 mL of distilled water to make a 0.1 M solution. This solution was then added to the dispersed CeO_2 solution and sonicated for 1 h. Next, 2.400 g of $Na_2S{\cdot}9H_2O$ was dissolved in 100 mL of distilled water to make a 0.1 M solution, which was added dropwise to the mixture, and sonication was continued for another hour to allow the precipitate to form. The product was then filtered and washed three times each with ethanol and distilled water. Finally, the composite was dried in an oven at 60 °C for 24 h, yielding the CdS/CeO_2 composite.

Preparation of ternary $CdS/CeO_2/Ag_2CO_3$ composites

The ternary composite catalysts with various weight ratios of CdS: CeO_2/Ag_2CO_3 (1:1, 2:1, 3:1, and 4:1) were synthesized by using a constant amount of prepared CeO_2/Ag_2CO_3 powder and varying amounts of the precursors $Cd(CH_3COO)_2{\cdot}2H_2O$ and $Na_2S{\cdot}9H_2O$ for CdS synthesis. In a typical procedure, for the weight ratio CdS: CeO_2/Ag_2CO_3 (3:1), 0.50 g of CeO_2/Ag_2CO_3 powder (0.1 M) was dispersed in 11.2 mL of deionized water and sonicated for 2 h, forming solution 1. Separately, 0.890 g of $Cd(CH_3COO)_2{\cdot}2H_2O$ (0.1 M in 33.4 mL) and 0.80 g of $Na_2S{\cdot}9H_2O$ (0.1 M in 33.4 mL) were prepared, labeled solutions 2 and 3, respectively. Solution 2 was added dropwise into solution 1 and sonicated for an additional 1.5 h. Then, solution 3 was added dropwise to the mixture of 1 and 2 while stirring continuously for 3 h. After filtration, the product was washed three times with ethanol and deionized water, then dried for 12 h at 80 °C, then labeled as $CdS/CeO_2/Ag_2CO_3$(3:1) ternary nanocomposite. The same procedure was followed for the remaining three weight ratios (1:1, 2:1, and 4:1), with the corresponding solutions prepared similarly maintaining the required stoichiometry (Fig. 1). The final powders were ground to fine particles and labeled as $CdS/CeO_2/Ag_2CO_3$(1:1), $CdS/CeO_2/Ag_2CO_3$(2:1), and $CdS/CeO_2/Ag_2CO_3$(4:1), respectively.

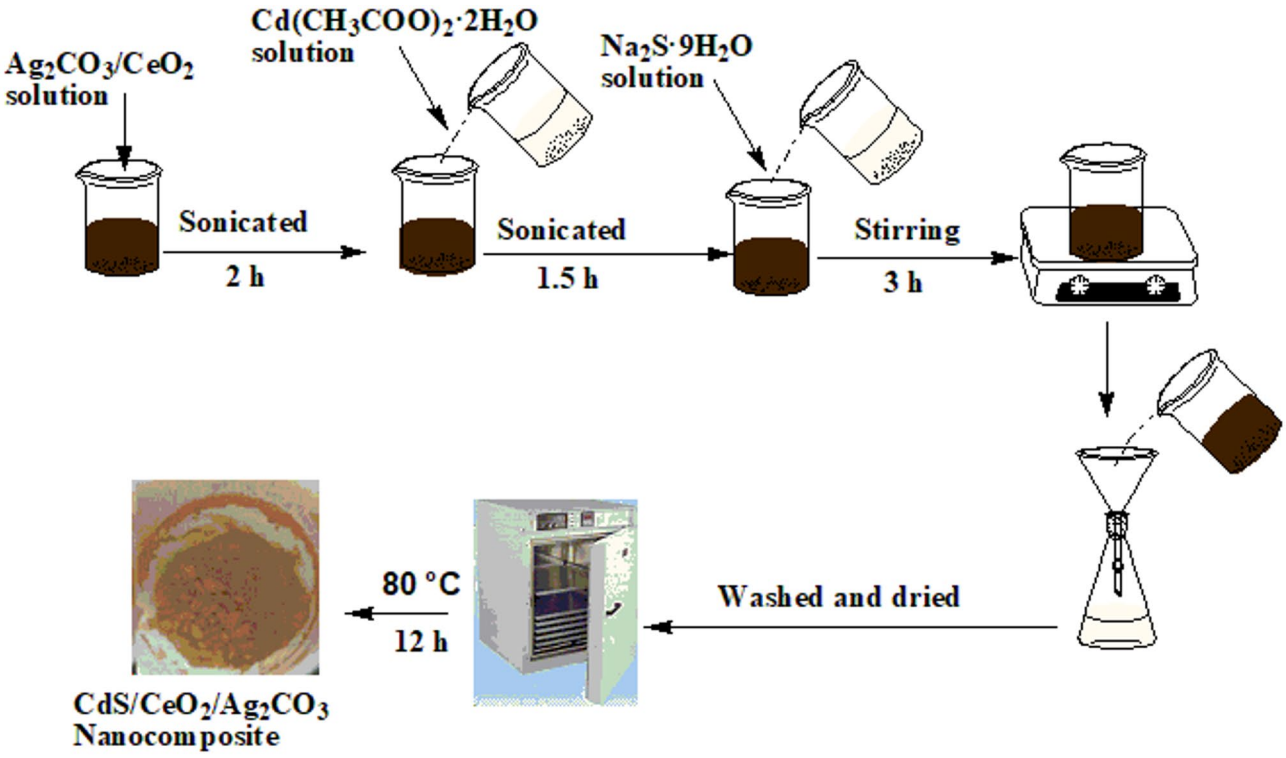

Fig. 1. The synthesis procedure for the ternary $CdS/CeO_2/Ag_2CO_3$ nanocomposite.

Characterization of synthesized materials

The phase purity and crystalline structure of the developed catalysts were characterized by Powder X-ray Diffraction (PXRD) using an X'Pert Pro PANalytical instrument, equipped with a Cu Kα radiation source (λ = 0.15406 nm). The XRD measurements were conducted with a scan rate of 0.02 (step time: 1 s) in the 2θ range of 5.0° to 90.4°. The surface composition and morphology of the prepared catalysts were analyzed using scanning electron microscopy (SEM) coupled with Energy Dispersive X-ray spectroscopy (EDX), employing a Hitachi Tabletop Microscope TM1000 with a tungsten filament electron gun. The functional groups of the prepared materials were investigated by Fourier Transform Infrared Spectroscopy (FTIR, Perkin Elmer) in the 400–4000 cm^{-1} range using the KBr disk method. The solid-state optical absorption spectrum of the catalysts was recorded using a UV-Vis spectrophotometer, scanning over the wavelength range of 200–900 nm. Nitrogen sorption isotherms were obtained at -196 °C using a Micromeritics ASAP 2420 instrument, and the surface area was calculated using the Brunauer-Emmett-Teller (BET) method.

Procedure for Knoevenagel condensation reaction

To begin the reaction, 2.0 mmol of aromatic aldehyde, 2.0 mmol of malononitrile, reaction time for 33 min, 10% w/w of the prepared nanocatalyst (relative to both reagents), and 5 mL of water were added to a 100 mL three-neck round-bottom flask. The reaction mixture was magnetically stirred at room temperature, and the progress was monitored using thin-layer chromatography (TLC) with a mobile phase of ethyl acetate and hexane in a 1:4 ratio. Once the reaction was complete, the product mixture was dissolved in methanol, and the catalyst was separated by filtration. The organic phase was then dried over anhydrous sodium sulfate. The methanol solvent was evaporated at room temperature, and the product was recrystallized from methanol to obtain the desired product.

Catalytic recyclability

The reusability of the $CdS/CeO_2/Ag_2CO_3$(1:3) catalyst for the Knoevenagel condensation reaction between benzaldehyde and malononitrile was assessed by evaluating the yield over multiple cycles, with reference to the first run. Briefly, the catalyst was separated from the reaction mixture by filtration at the end of each cycle. It was then washed several times with deionized water and absolute ethanol. Afterward, the catalyst was dried at 100 °C and reused in the subsequent run with fresh reactants under the same reaction conditions.

General procedure for acetylation

In a standard procedure for the acetylation of an amine, 2.0 mmol of aromatic amine, 2.0 mmol of acetic anhydride, under 3 min reaction time, and 10% w/w of the prepared $CdS/CeO_2/Ag_2CO_3$(1:3) nanocatalyst (relative to the total reagents) were added to a three-neck round-bottom flask at room temperature, following a previously reported method with slight modifications[40]. The reaction mixture was magnetically stirred, and the reaction progress was monitored by TLC using a mobile phase with a 1:4 ratio of ethyl acetate to hexane. Once the reaction was complete, the product mixture was dissolved in 10 mL of ethyl acetate, and the catalyst was separated by simple filtration. The organic phase was then washed with a 10% $NaHCO_3$ solution in a separatory funnel, and the upper layer was dried over anhydrous Na_2SO_4. Finally, ethyl acetate was evaporated, and the desired product was collected.

Results and discussion

Catalyst characterization

XRD analysis

Fig. 2 shows the XRD patterns of the as-prepared single component materials (Ag_2CO_3, CdS, and CeO_2), binary composites (Ag_2CO_3/CeO_2 and CdS/CeO_2), and ternary composites with different CdS: CeO_2/Ag_2CO_3 molar ratios (1:1, 2:1, 3:1, and 4:1). The diffraction peaks of Ag_2CO_3 are sharp and align well with previously reported data [96-100-7036][41]. The broad diffraction peaks observed at 2θ values of 26.88°, 44.23°, and 51.95° correspond to a hexagonal greenockite CdS structure [96-900-8863][42]. CeO_2 patterns display intense diffraction peaks at 2θ values of 28.44°, 33.02°, 47.37°, 56.23°, 59.00°, 69.33°, 76.42°, 79.06° and 88.47°, which are described the cubic fluorite CeO_2 structure [JCPDS: 96-900-9009][43]. For the binary nanocomposites, the XRD patterns of Ag_2CO_3, CdS, and CeO_2 can be clearly identified without any impurities [44]. However, intense diffraction peaks ascribed to cubic fluorite CeO_2 structure are observed in CdS/CeO_2 system, while weak diffraction peaks at 26.60°, 44.00°, and 51.70° are attributed to the hexagonal greenockite CdS structure[45].

The XRD patterns of the as-prepared $CdS/CeO_2/Ag_2CO_3$ ternary composites, featuring various molar ratios of CdS to CeO_2/Ag_2CO_3 (1:1, 2:1, 3:1 and 4:1), showed the distinct presence of the individual components: CeO_2, Ag_2CO_3, and CdS within the ternary systems. The XRD results demonstrated that the as-prepared pristine, binary, and ternary composite materials were successfully synthesized with no trace of any impurity.

The average crystallite sizes of as-prepared catalysts were calculated using the Debye-Scherrer formula as shown in Eq. (1):

$$D = (k\lambda) / (\beta \cos\theta) \quad (1)$$

Where β is the full width at half maximum (FWHM) in radians, λ is the wavelength of the X-ray (0.15406 nm) for Cu target Kα1 radiation, θ is the Bragg's angle in radians, D is the crystallite size in nm. k is the shape factor constant, which is taken to be 0.9. Table S1 shows the average crystallite size of each as-prepared catalyst. Smaller crystallite sizes typically result in a higher specific surface area and a great number of active sites, boosting the

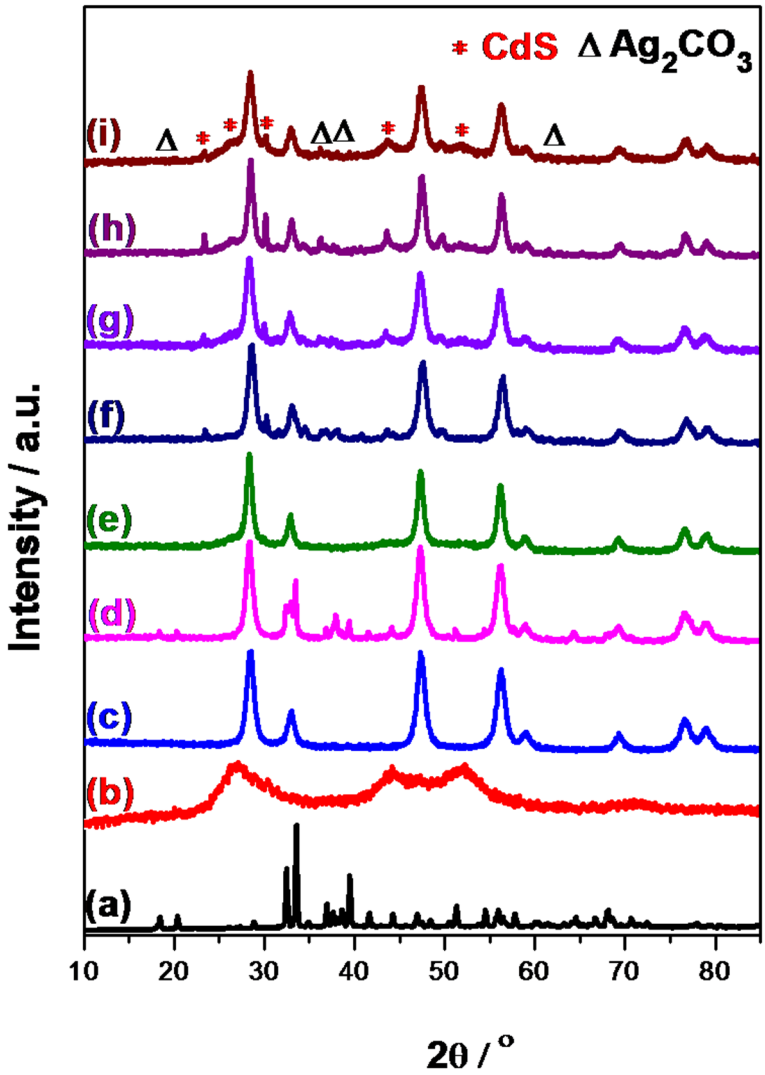

Fig. 2. XRD patterns of (a) Ag_2CO_3, (b) CdS, (c) CeO_2, (d) Ag_2CO_3/CeO_2, (e) CdS/CeO_2, (f) $CdS/CeO_2/Ag_2CO_3$ (1:1), (g) $CdS/CeO_2/Ag_2CO_3$ (2:1), (h) $CdS/CeO_2/Ag_2CO_3$ (3:1), and (i) $CdS/CeO_2/Ag_2CO_3$ (4:1) samples.

catalytic performance in Knoevenagel condensation and acetylation reactions by improving reactant adsorption and faster reaction kinetics.

SEM analysis

The SEM images of the as-prepared pristine, binary, and ternary composite materials are shown in Fig. 3a-j. The Ag_2CO_3 (Fig. 3a-b) exhibits a homogeneous spherical shape, while CdS (Fig. 3c-d) displays an irregular form due to numerous aggregated nanosized particles. CeO_2 (Fig. 3e-f) is characterized by nano-stick shapes, with average edge length in the micrometer range. The spherical, irregular, and nano-stick morphologies enhance catalytic performance by increasing active site availability, providing defect-driven active sites, and improving mass transport, respectively, maximizing surface area, reactant accessibility, and efficiency. The SEM images for both the binary (Fig. 3g-i) and ternary composite (Fig. 3j) shows the existence of interactions among the various components. In addition, the SEM-EDS spectrum of ternary $CdS/CeO_2/Ag_2CO_3$ composite confirmed the presence of Ce, Cd, Ag, S, and O atoms (Fig. 3k).

Analysis of N_2 sorption isotherms

Fig. 4 shows the N_2 adsorption/desorption isotherms of $CdS/CeO_2/Ag_2CO_3$ (3:1) at -196 °C. The BET specific surface area of the as-prepared $CdS/CeO_2/Ag_2CO_3$(3:1) was 75.33 m^2g^{-1}, which is higher than the previously reported value of CeO_2 nanoparticles (72.9 m^2 g^{-1})[46]. The increased specific surface area boosts active site availability for reactant adsorption, crucial for surface reactions, while also promoting better distribution of active components (CdS, CeO_2, and Ag_2CO_3), improving interfacial interactions and catalytic efficiency[47].

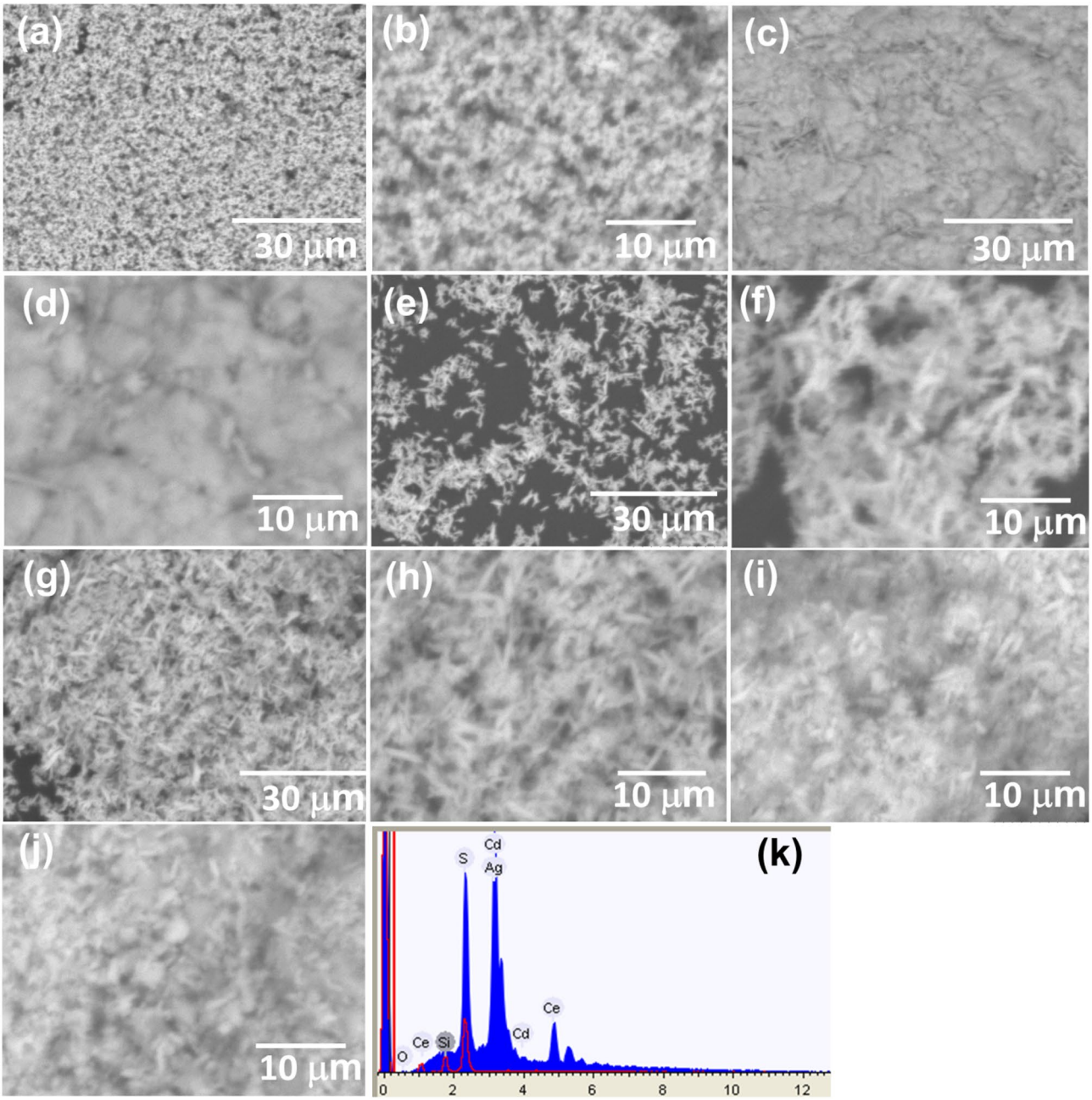

Fig. 3. SEM images of (a-b) Ag_2CO_3, (c-d) CdS, (e-f) CeO_2, (g-h) Ag_2CO_3/CeO_2, (i) CdS/CeO_2, (j) $CdS/CeO_2/Ag_2CO_3$(3:1) and (k) EDS analysis of ternary $CdS/CeO_2/Ag_2CO_3$(3:1) samples.

Fourier transform infrared (FT-IR) spectroscopy

The functional groups of as-prepared catalysts were analyzed using FT-IR spectroscopy (from 400 to 4000 cm^{-1}) as demonstrated in Fig. 5. The wide peaks at 3399 and 1620 cm^{-1} represents stretching and bending vibration of O-H bond and the peak at 1054 cm^{-1} also indicate the existing of C-O on the surface of catalyst that could be associated with adsorbed CO_2 [41,44]. As depicted in Fig. 5(a), the lowest intense peak at 1544 cm^{-1} is recognized to the asymmetric stretching vibration of -COO- obtained from ionized carboxylate groups served as linker for the synthesis of Ce-MOF. The peak at 543 cm^{-1} corresponds to the Ce-O stretching vibration of CeO_2 [45]. In contrast, the smaller bands at 2922, 2854, and 722 cm^{-1} are attributed to the to the asymmetrical and symmetrical C-H stretching vibrations, as well as the C-H out-of-plane bending vibrations, resulting from the ethanol solvent used[46]. The band at 1330 and 850 cm^{-1} can be ascribed to N = O symmetrical stretching and the stretching of the pi (Π) bonds of the N-O bond that existing from $Ce(NO_3)_3.6H_2O$ used[48].

As shown in Fig. 5(b), the peak at 1405 cm^{-1} refer to stretching vibration of CO_3^{-2}[49] and the band at 520 cm^{-1} indicate the presence of Ce-O in composite materials. But the wavenumber (520 cm^{-1}) is lower than pure Ce-O (543 cm^{-1}), which indicates the shifting of absorption to lower energy in binary composite system.

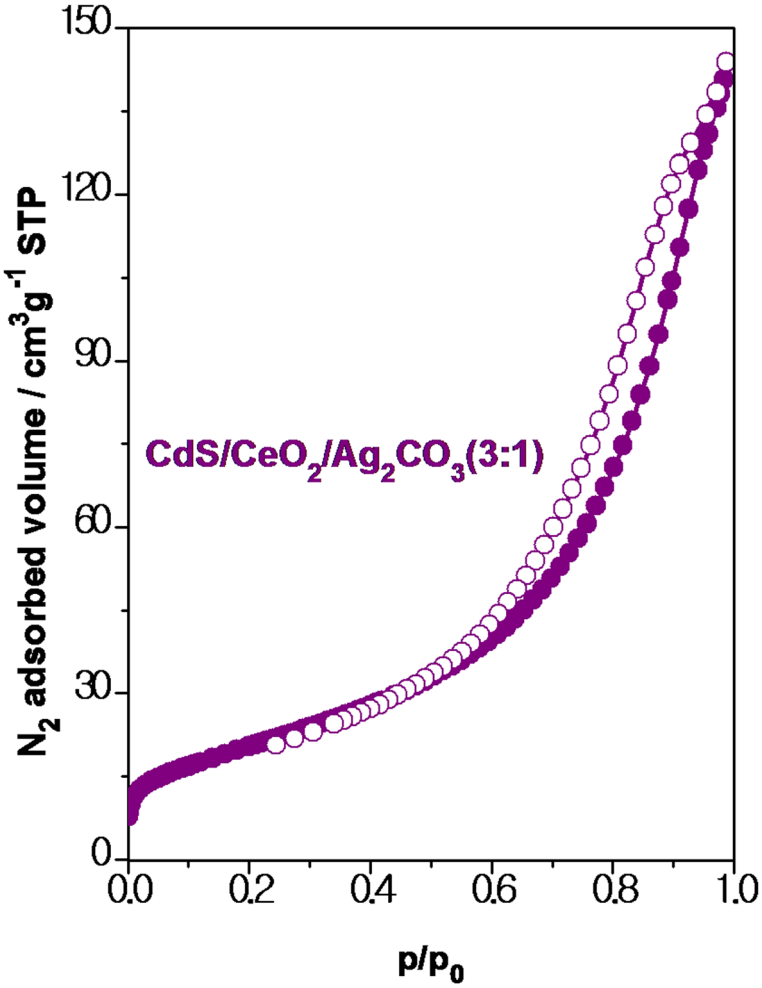

Fig. 4. N_2 adsorption-desorption isotherms at -196 °C (activated at 150 °C for 16 h) of $CdS/CeO_2/Ag_2CO_3$ (3:1) sample.

The absorption peaks at 658 and 617 cm^{-1} indicated the vibrational stretching of Cd-S (Fig. 5c). Subsequently, the absorption band at 535 cm^{-1} is recognized the presence of Ce-O in composite and it has been slightly smaller wavenumber than single CeO_2 particles due to the effect of intrinsic behavior of CdS. In the case of ternary composite that depicted in Fig. 5(d), the pecks at 1403, 653, 618, and 534 cm^{-1} could be attributed to stretching vibration of CO_3^{-2}, vibrational stretching of Cd-S, stretching vibration of S-S, and Ce-O stretching vibrations respectively.

UV-Vis diffuse reflectance absorption

The absorption spectra of as-prepared catalysts are depicted in Fig. 6(a-f). The absorption edges of binary and ternary composites were extended to visible wavelength region compared to CeO_2 nanoparticles. The systematic coupling of CdS and Ag_2CO_3 nanoparticles in the composite enhances the optical properties, facilitating the activation of surface-adsorbed reactants and intermediates by improving charge carrier generation, as illustrated in the reaction mechanism. This accelerates reaction kinetics by facilitating nucleophilic attack and subsequent condensation, increases the overall catalytic efficiency, and leads to higher yields and faster reaction rates in Knoevenagel condensation and acetylation reactions[50] This evidences the formation of a unique heterojunction in the ternary nanocomposite.

Catalytic study for Knoevenagel condensation

Optimization of reaction conditions

The Knoevenagel condensation reaction can be efficiently aided by a variety of acid-base bifunctional Lewis acids that concurrently activate the carbonyl group at acid sites and deprotonate from malononitrile at basic sites[18,24,47]. Thus, the synthesized $CdS/CeO_2/Ag_2CO_3$ (3:1) ternary nanocatalyst was used to study the catalytic potential in the Knoevenagel condensation reaction. Fig. 7 illustrates the optimization of reaction conditions using malononitrile and benzaldehyde as a substrate. The effects of solvent, catalyst quantity, and reaction temperature were examined and optimized in order to achieve an ideal reaction condition as shown in Table 1.

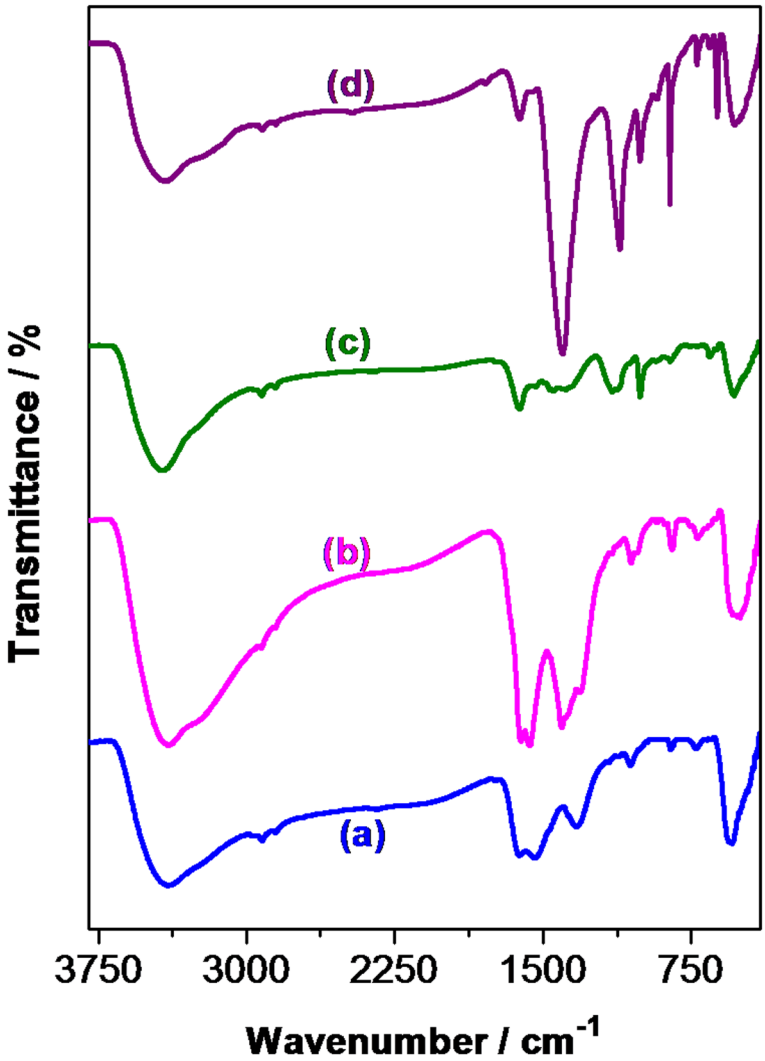

Fig. 5. FTIR spectra of (a) CeO_2, (b) Ag_2CO_3/CeO_2, (c) CdS/CeO_2, and (d) $CdS/CeO_2/Ag_2CO_3$ (3:1) samples.

Effect of solvent The impact of various solvents on the catalytic activity of $CdS/CeO_2/Ag_2CO_3$ (3:1) for model reaction was examined in Table 1 (entry1-8). The reaction was conducted through benzaldehyde (2.0 mmol) and malononitrile (2.0 mmol), at room temperature and catalyst amount was set at 10%, w/w of total reagent weight. Utilizing a heterogeneous catalyst, the Knoevenagel condensation reaction process has been reliant on the polarity of solvent's reaction[20,51]. The use of solvent free condition or solvent like acetonitrile, toluene, dichloromethane and chloroform gave a low yield at longer reaction time. The use of ethanol and methanol produced good yield. To establish an environmentally friendly solvent, water was identified as the optimal choice for the reaction, achieving a yield of 92.19 ± 0.41% in just 33 min (Table 1, entry 5). Using water as a solvent offers numerous advantages, including its cost-effectiveness, abundance, safety, and non-toxicity. It simplifies the synthesis process by allowing for easy precipitation without the need for lengthy quenching, while also mitigating issues related to self-condensation.

Catalyst amount The effects of catalyst dosage on the reaction rate and yield of the model reaction were evaluated using various amount (0–20%, w/w of total reagent weight) of $CdS/CeO_2/Ag_2CO_3$ (3:1) at room temperature in water (Table 1, entry 9–17). The optimal catalyst load of 10% w/w achieved a yield of 92.19 ± 0.41% in just 33 min (Table 1, entry 13). In contrast, the reaction without the catalyst resulted in a minimal yield of 39.94 ± 1.81% at 377 min (Table 1, Entry 9). Using lower quantities than the optimal load (2.5, 5, and 7% w/w) improved yield and reduced reaction time (Table 1, entry 10–12). However, increasing the catalyst load beyond the optimal level to 20% w/w led to a decrease in yield and an increase in reaction time, likely due to agglomeration and other factors.

Reaction temperature The impact of reaction temperature on the selected model reaction was examined from 20 to 120 °C at 20 °C intervals (Table 1, entry 18–23). The results indicated a 1% increase in yield of 2-benzylidenemalononitrile at 60 °C (Table 1, entry 20). However the reaction time and yield did not significantly

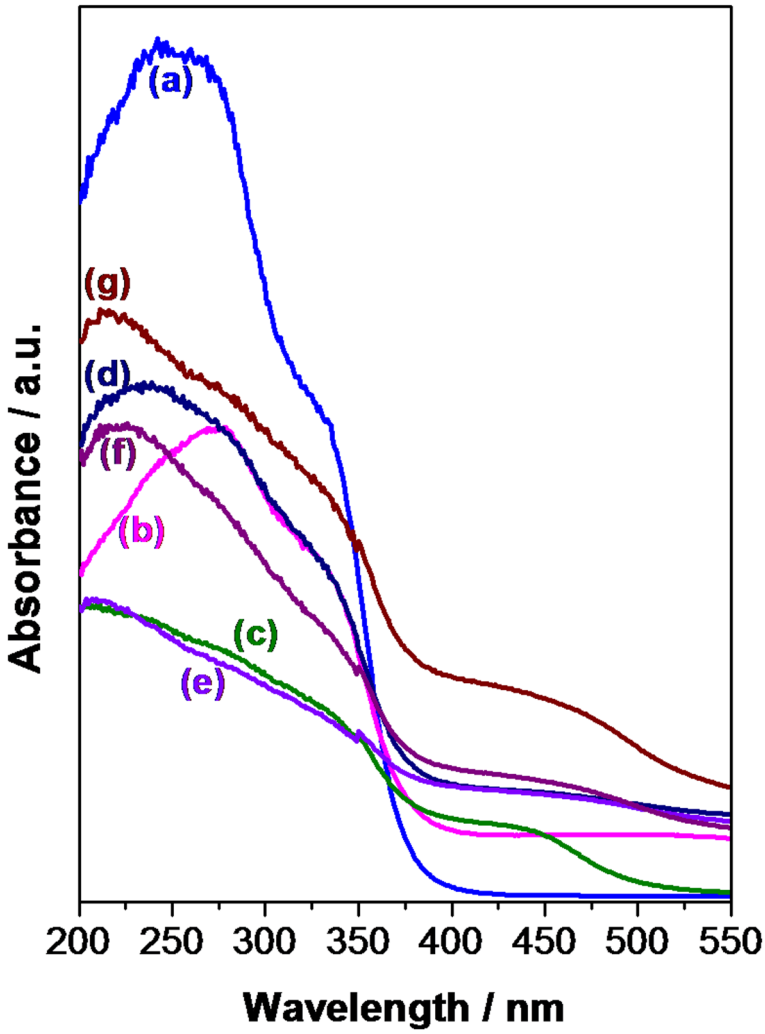

Fig. 6. DR-UV-vis spectra of (a) CeO_2, (b) Ag_2CO_3/CeO_2, (c) CdS/CeO_2, (d) $CdS/CeO_2/Ag_2CO_3$(1:1), (e) $CdS/CeO_2/Ag_2CO_3$(2:1), and (f) $CdS/CeO_2/Ag_2CO_3$(3:1) samples.

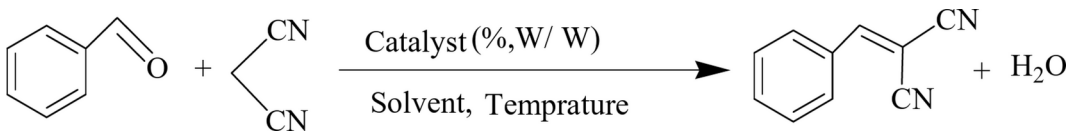

Fig. 7. Knoevenagel condensation reaction using prepared catalyst.

change between 20 and 40 °C. Considering environmental conditions and eco-friendliness, 20 °C was chosen as the optimal reaction temperature. Notably, temperatures of 80 ° C and above resulted inlow yields despite faster reaction times.

Comparison of synthesized catalytic efficiency for Knoevenagel condensation

After optimizing the reaction condition using $CdS/CeO_2/Ag_2CO_3$ (3:1) for the Knoevenagel reaction of benzaldehyde with malononitrile, we compared the synthesized catalysts: CeO_2, CdS/CeO_2, Ag_2CO_3/CeO_2, and the ternary $CdS/CeO_2/Ag_2CO_3$ composites (1:1, 2:1, and 4:1). These comparisons were conducted at room temperature, using water as the solvent and a catalyst load of 10% w/w, as presented in Table 2, entry 1–7. The results indicated that the catalytic performance of as-prepared single, binary and ternary catalysts improved in the following order: $CdS/CeO_2/Ag_2CO_3$ (3:1) > $CdS/CeO_2/Ag_2CO_3$ (4:1) > $CdS/CeO_2/Ag_2CO_3$ (2:1) > $CdS/CeO_2/Ag_2CO_3$ (1:1) > CdS/CeO_2 > Ag_2CO_3/CeO_2 > CeO_2 , with respect to both yield and reaction time. As seen in Table 2, the enhancement of catalytic performance from a single to binary to ternary catalyst makes it clear that coupling create a diverse active sites environment from the heterostructures, which improves the conversion efficiency. This may be explained by the small crystallite size (Table S1) than binary composites and

Entry	Catalyst (%)	Solvent	Temperature (°C)	Time (min)[a]	Yield (%)[b]
1	10	Neat	20	51	83.24± 0.47
2	10	Ethanol	20	41	89.01± 1.76
3	10	Methanol	20	36	89.90± 1.39
4	10	Acetonitrile	20	103	70.40± 1.31
5	10	Water	20	33	92.19± 0.41
6	10	Toluene	20	90	68.47± 2.63
7	10	Dichloromethane	20	115	63.63± 1.41
8	10	Chloroform	20	126	62.03± 2.12
9	Blank	Water	20	377	39.94 ± 1.81
10	2.5	Water	20	57	72.75± 2.10
11	5	Water	20	42	84.93 ± 2.15
12	7.5	Water	20	38	86.85± 1.43
13	10	Water	20	33	92.19± 0.41
14	12.5	Water	20	37	91.80 ± 1.21
15	15	Water	20	49	85.47± 1.62
16	17.5	Water	20	67	85.15± 2.19
17	20	Water	20	74	81.39± 1.96
18	10	Water	20	33	92.19± 0.41
19	10	Water	40	31	92.45± 1.69
20	10	Water	60	32	93.18± 1.71
21	10	Water	80	28	92.55± 2.07
22	10	Water	100	28	92.55± 1.86
23	10	Water	120	28	92.36± 2.41

Table 1. Optimization of reaction condition. Reaction conditions, [a]Monitored by TLC, [b]Isolated yield, benzaldehyde (2 mmol), malononitrile (2 mmol), temperature (°C), solvent (5 mL), catalyst (% w/w of total reagent weight) and reaction repeating three times.

Entry	Nanocatalyst	Time (min)[a]	Yield (%)[b]
1	CeO_2	115	70.20± 1.55
2	CdS/CeO_2	72	80.63± 1.23
3	Ag_2CO_3/CeO_2	89	73.49± 1.41
4	$CdS/CeO_2/Ag_2CO_3$ (1:1)	71	81.11± 1.74
5	$CdS/CeO_2/Ag_2CO_3$ (2:1)	53	85.32± 2.23
6	$CdS/CeO_2/Ag_2CO_3$ (3:1)	33	92.19± 0.41
7	$CdS/CeO_2/Ag_2CO_3$ (4:1)	63	87.48± 1.69

Table 2. Comparison of the catalytic performance of synthesized nanocatalysts for reaction of benzaldehyde and malononitrile. Reaction conditions, [a]Monitored by TLC, [b]Isolated yield, benzaldehyde (2 mmol), malononitrile (2 mmol), temperature (20 °C), H_2O (5 mL), catalyst (% w/w of total reagent weight) and reaction repeating three times.

has a high catalytic activity due to large available active sites[22,52]. After demonstrating superior efficacy over the other catalytic system, the ternary catalyst was nominated for further investigation. Therefore, ternary $CdS/CeO_2/Ag_2CO_3$ (3:1) system was the most effective composite which produced a yield of 92.19 ± 0.41% with a reaction time of only 33 min (Table 2, entry 6) than other counterparts.

Reaction scope

The catalytic efficiency of $CdS/CeO_2/Ag_2CO_3$ (3:1) for Knoevenagel condensation reaction of various aromatic aldehydes with malononitrile was evaluated under optimal conditions (water as solvent, room temperature, and 10% w/w catalyst load) (Table 3, entry 1–5). Electron donating substituents enhance the electron concentration the carbonyl group[20,24,53], resulting in a yield of 76.97 ± 1.53% for 4-dimethylaminobenzaldehyde in 53 min (Table 3, entry 5). However, the efficiency wast slightly lower with other electron-donating groups, such as 4-hydroxyl and 3, 4, 5-methoxy (Table 3, entry 3–4). In contrast, the electron withdrawing group 2-nitrobenzaldehyde exhibited high conversion and better yield compared to the donating groups (Table 3, entry 1). For 3-nitrobenzaldehyde, the product yield decreased due to the lack of resonance stabilization at this position (Table 3, entry 2).

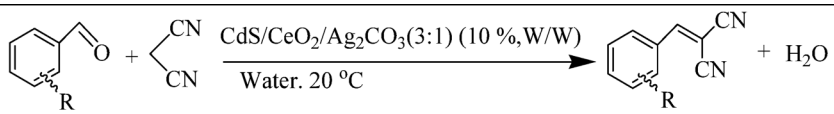

Entry	R	Product	Time (min)[a]	Yield (%)[b]	Melting point (°C)		
					Measured	Reported	Ref
1	H	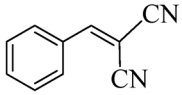	33	92.19± 0.41	83-84	81-83	54
2	2-NO_2	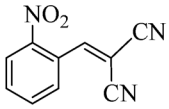	29	92.70± 1.02	136-137	136-138	55
3	3-NO_2	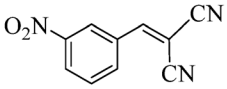	44	88.66± 1.73	101-103	102-103	54
4	4-OH	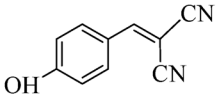	47	89.33± 1.99	187-189	186-187	56
5	3,3,4-OCH_3	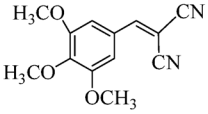	46	86.59± 1.09	135-136	136	57
6	4-$N(CH_3)_2$	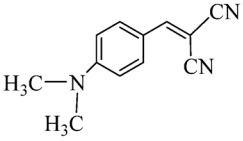	53	76.97± 1.53	181-182	180-182	58

Table 3. Knoevenagel condensation of aromatic aldehydes with malononitrile catalyzed by $CdS/CeO_2/Ag_2CO_3$ (3:1)[a].
Reaction conditions, [a]Monitored by TLC, [b]Isolated yield, aromatic benzaldehyde (2 mmol), malononitrile (2 mmol), temperature (20 °C), H_2O (5 mL), $CdS/CeO_2/Ag_2CO_3$ (3:1) catalyst (% w/w of total reagent weight) and reaction repeating three times.

Entry	Catalyst	Reaction Condition	Time	Yield (%)	Ref.
1	$Ce_xZr_{1-x}O_2$	Ethanol, 80 °C	50 min	82	47
2	Al_2O_3-SiO_2-MgO	Ethanol, RT	90 min	91	59
3	$BaAl_2O_4$	Ethanol, RT	10 h	80	60
4	ZnO	Neat, RT	3.5 h	90	61
5	Fe_3O_4@ZIF-8	Toluene, RT	3 h	94	62
6	$CdS/CeO_2/Ag_2CO_3$(3:1)	Water, RT	33 min	92.19± 0.41	This study

Table 4. Comparison of $CdS/CeO_2/Ag_2CO_3$(3:1) for reaction between benzaldehyde and malononitrile with previous reported.

Comparison with different reported catalysts for Knoevenagel condensation reaction
comparison of catalytic efficiency between the $CdS/CeO_2/Ag_2CO_3$(3:1) ternary nanocatalyst and previously reported catalysts for the Knoevenagel condensation reaction is presented in Table 4. This table highlights the advantages of the ternary nanocatalyst in terms of yield and reaction time, showcasing its effectiveness realative to other catalysts in the literature. It was found that the present catalyst is advantageous in terms of low temperature, simplicity and cost-effectiveness, water as a solvent and recyclability. Furthermore, it takes low reaction time in a mild condition as compared with the previous reported in Table 4.

Proposed mechanism of Knoevenagel condensation reaction

The surface composition of $CdS/CeO_2/Ag_2CO_3$(3:1) catalyst has Lewis's acid-base active sites like other metal oxide catalyst[63]. Fig. 8 shows that the plausible reaction mechanisms in between benzaldehyde and malononitrile using the selected catalyst. In the first step, the Lewis acid site of the catalyst (Ce^{4+}, Cd^{2+} and Ag^{+}) adsorbs and interacts with the benzaldehyde's carbonyl group, giving the carboxylic active electrophilic character. At the same time, the Lewis base site (O^{-2}, S^{-2} and CO_3^{-2}) removes the acidic proton from the malononitrile's methylene group and creates a carbanion. In the next step the activated carbonyls undergo nucleophilic attack by carbanion with double bond formation. In the later stage, extrusion occurs, resulting in the condensed product while facilitating the removal of water. Additionally, catalyst recycling takes place during this final stage, allowing for efficient reuse of the catalyst in subsequent reactions.

Recyclability of $CdS/CeO_2/Ag_2CO_3$ (3:1) for Knoevenagel condensation reaction

One of the most important requirements for the synthesis of organic products using heterogeneous catalysis is the catalyst's ability to be recycled[21,64]. Due to this, the reusability of present catalyst was conducted by performing a series of repetitive experiments for reaction of benzaldehyde with malononitrile at optimal reaction conditions. The catalyst was employed for the subsequent comparable run after being quickly recovered from the reaction mixture by filtration, methanol washing, and dried at 60 °C. Our findings revealed that the catalyst can be recycled up to six times, maintaining a good catalytic efficiency with a yield of 85.79 ± 1.21%. This reflects an overall drop of only 6.70%, demonstrating the catalyst's stability and effectiveness over multiple uses. While the catalytic activities of the first through fifth cycles are as follows: 92.19 ± 0.41, 90.81 ± 0.99, 89.73 ± 1.13, 87.96 ± 0.86, 87.07 ± 1.28, and 85.79 ± 1.21%, respectively. The material demonstrates excellent stability, as confirmed by the XRD patterns before and after the catalytic tests (Fig. S2). These experimental results suggest that the selected catalyst has high reusability or durability for the Knoevenagel condensation reaction. The turn over number (TON) and turn over frequency (TOF) of Knoevenagel condensation reaction is 32 and 56 h^{-1} respectively.

Catalytic study of $CdS/CeO_2/Ag_2CO_3$ (3:1) for acetylation

After conformation of $CdS/CeO_2/Ag_2CO_3$(3:1) ternary nanocomposite was an efficient catalyst for Knoevenagel condensation reaction, we improved the catalytic efficiency of the present catalyst for further acetylation reaction based on previous report at room temperature and solvent free reaction condition[40]. The outcome of reaction of aniline derivatives with acetic anhydride was depicted in Table 5, entry 1–7. Surprisingly, acetylation of aniline was completed in just 3 min with achieved 93.80 ± 1.19% yield (Table 5, entry 1). The presence of electron

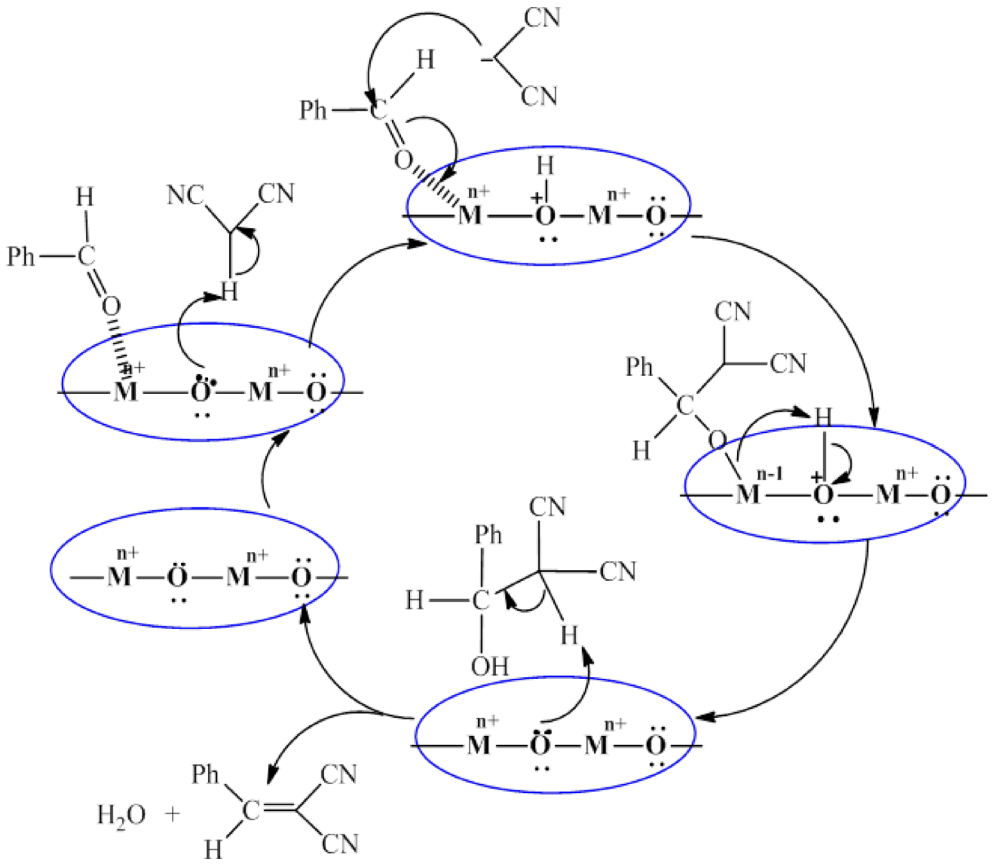

Fig. 8. Plausible mechanism of Knoevenagel condensation reaction.

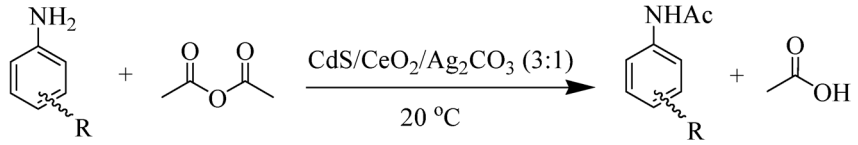

Entry	R	Product	Time[a] (min)	Yield[b] (%)	Melting point (°C)	Ref.
1	H	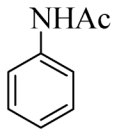	3	93.8± 1.19	114 -115	113-115 [65]
2	3-Cl	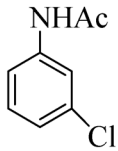	15	87.7± 0.59	74 -77	77-78 [66]
3	4-Cl	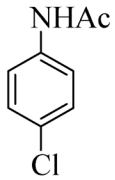	15	89.7± 1.08	180 -181	179-181 [65]
4	2-NO_2	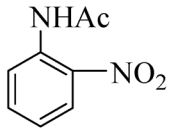	14	84.8± 0.89	89 -92	92-94 [67]
5	4-NO_2	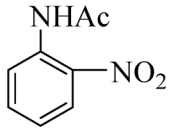	11	87.0± 1.09	212-214	214-216 [68]
6	3-NO_2	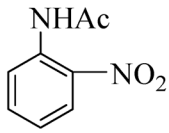	12	90.8± 1.39	152-156	152-154 [69]

Table 5. Acetylation of aniline derivatives using $CdS/CeO_2/Ag_2CO_3$ (3:1)[a].
Reaction conditions, [a]Monitored by TLC, [b]Isolated yield, aniline (2 mmol), acetic anhydride (2 mmol), neat reaction, catalyst (10% w/w of total reagent) and temperature (20 °C).

withdrawing substituents, such as -Cl and -NO_2 slightly decreases the reaction yield, likely due to their effect on reducing the nucleophilicity of aniline (Table 5, entry 2–5). However, the reaction with 3-nitroanilinedid not exhibit a significant change in yield (Table 5, entry 6), possibly becausethere is not resonance stabilization factor for this aniline. The turnover number (TON) and turnover frequency (TOF) for the acetylation reaction were measured at 28 and 569 h^{-1}, respectively.

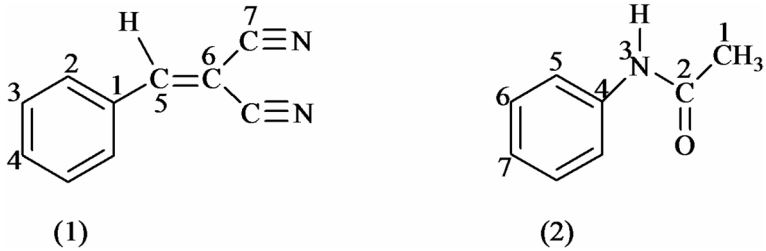

Fig. 9. The as-synthesized organic products of (1) 2-benzylidinemalononitrile and (2) acetanilide product.

Characterization of synthesized 2-benzylidinemalononitrile and acetanilide

The purity and conversion of as-synthesized organic products were checked using TLC method (Fig. S1) with their melting point. Beside to these, the structural identity of 2-benzalidinemalononitrile (Fig. 9(1) and acetanilide (Fig. 9(2) product was confirmed using FTIR (Figs. S3-S4),^{1}H-NMR (Figs. S5 and S7) and^{13}C-NMR (Figs. S6 and S8) at $CDCl_3$ solvent.

2-Benzalidinemalononitrile (Fig. 9(1))

Solid state, white color, FTIR (Fig. S3) (KBr, cm^{-1}) 3412, 3012, 2923, 2849, 2223, 1593, 1568, 1450, 1380, 756, 679, 618, 519;^{1}H-NMR (Fig. S5) (400 MHz, $CDCl_3$): δ_H (ppm) 7.81(1 H, s, H5), 7.92(2 H, d, H2), 7.56(2 H, t, H3), 7.66 (1 H, t, H4);^{13}C-NMR (Fig. S6) (100.6 MHz, $CDCl_3$): δ_C (ppm) 82.74(C6), 112.65–113.80(C7), 129.68-130.95(C2,C3, C4), 134.72 (C1) and 160.13(C5).

Acetanilide (Fig. 9(2))

Solid state, white color, FTIR (Fig. S4) (KBr, cm^{-1}) 3296, 3059–3192, 2802, 1666, 1558–1597, 1435, 1269–1369, 907–1011, 759, 694 ,510;^{1}H-NMR (Fig. S7) (400 MHz, $CDCl_3$): δ_H (ppm) 2.18(3 H, s, H1), 7.79 (1 H, s,H2), 7.52 (2 H, d,H5), 7.32(2 H, t,H6), 7.12(1 H, t,H7);^{13}C-NMR (Fig. S8) (100.6 MHz, $CDCl_3$): δ_C (ppm) 24.53(C1), 168.72(C2), 137.97(C4), 128.96(C6), 124.31(C7) and 120.03(C5).

Conclusions

In conclusion, we developed a new catalyst, the $CdS/CeO_2/Ag_2CO_3$ (3:1) ternary nanocomposite, for the Knoevenagel condensation reaction of aromatic aldehydes with an active methylene compound of malononitrile. We also designed, characterized, and investigated the effectiveness of this catalyst for the acetylation of aniline derivatives with acetic anhydride. The synthesis of this nanocatalyst was realized through the precipitation method. The current catalyst for two reactions was superior over convectional reported metal oxide nanocatalyst in terms of heterogeneous in nature, ambient reaction condition, fast rate of reactions, smallest loading catalyst, high yields of condensation and acetylation product with high TON and TOF values, as well as broad substrate scope. The prepared nanocatalyst also exhibited reusability up to six consecutive runs without notable decline in its efficiency, and its removal from the reaction mixture is as easy using filtration. In addition, the designed procedure is sustainable and green to easily collect the product of acetylation and Knoevenagel condensation reaction, cost effectiveness, nonhazardous chemical uses, solvent free for acetylation and water as solvent for Knoevenagel condensation. Electron-withdrawing groups (EWG) on the benzaldehyde derivatives tend to enhance the electrophilicity of the carbonyl carbon, making it more susceptible to nucleophilic attack by malononitrile. This generally leads to higher yields and shorter reaction times. Conversely, electron-donating groups (EDG) reduce the electrophilicity of the carbonyl carbon, resulting in relatively lower yields and longer reaction times due to decreased reactivity. We have included specific examples from our data to illustrate these trends, such as the higher yield and faster reaction observed with nitro-substituted benzaldehyde (an EWG) compared to methoxy-substituted benzaldehyde (an EDG).We trust that the created $CdS/CeO_2/Ag_2CO_3$ ternary nanocatalyst could have potential industrial applications for substantial organic conversion reactions under sustainable and environmentally friendly conditions.

Data availability

The data that support the findings of this study are available from the corresponding author Jemal M. Yassin, upon reasonable request.

Received: 30 December 2024; Accepted: 7 May 2025
Published online: 21 May 2025

References

1. Yao, C. et al. A cationic zinc–organic framework with Lewis acidic and basic bifunctional sites as an efficient solvent-free catalyst: CO_2 fixation and Knoevenagel condensation reaction. *Inorg. Chem.* **57**, 11157–11164. https://doi.org/10.1021/acs.inorgchem.8b01713 (2018).
2. Li, C. et al. Two organic–inorganic hybrid polyoxovanadates as reusable catalysts for Knoevenagel condensation. *New. J. Chem.* **43**, 5813–5819. https://doi.org/10.1039/C8NJ06460A (2019).

3. Joharian, M., Morsali, A., Tehrani, A. A., Carlucci, L. & Proserpio, D. M. Water-stable fluorinated metal–organic frameworks (F-MOFs) with hydrophobic properties as efficient and highly active heterogeneous catalysts in aqueous solution. *Green. Chem.* **20**, 5336–5345. https://doi.org/10.1039/C8GC02367K (2018).
4. Patel, D., Vithalani, R. & Modi, C. K. Highly efficient FeNP-embedded hybrid bifunctional reduced graphene oxide for Knoevenagel condensation with active methylene compounds. *New. J. Chem.* **44**, 2868–2881. https://doi.org/10.1039/C9NJ05821D (2020).
5. Jain, K., Chaudhuri, S., Pal, K. & Das, K. The Knoevenagel condensation using quinine as an organocatalyst under solvent-free conditions. *New. J. Chem.* **43**, 1299–1304. https://doi.org/10.1039/C8NJ04219E (2019).
6. Valentini, F., Galloni, P., Brancadoro, D., Conte, V. & Sabuzi, F. A stoichiometric solvent-free protocol for acetylation reactions. *Front. Chem.* **10**, 842190. https://doi.org/10.3389/fchem.2022.842190 (2022).
7. Scriven, E. F. 4-Dialkylaminopyridines: super acylation and alkylation catalysts. *Chem. Soc. Rev.* **12**, 129–161. https://doi.org/10.1039/CS9831200129 (1983).
8. Gholap, A. R., Venkatesan, K., Daniel, T., Lahoti, R. & Srinivasan, K. Ultrasound promoted acetylation of alcohols in room temperature ionic liquid under ambient conditions. *Green. Chem.* **5**, 693–696. https://doi.org/10.1039/B308069B (2003).
9. Bonner, T. & McNamara, P. The pyridine-catalysed acetylation of phenols and alcohols by acetic anhydride. *J. Chem. Soc. B.* 795–797. https://doi.org/10.1039/J29680000795 (1968).
10. Bartoli, G. et al. Per-O-acetylation of sugars catalyzed by Ce (OTf) 3. *Green. Chem.* **6**, 191–192. https://doi.org/10.1039/B400920G (2004).
11. Chakraborti, A. K. & Gulhane, R. Perchloric acid adsorbed on silica gel as a new, highly efficient, and versatile catalyst for acetylation of phenols, thiols, alcohols, and amines. *Chem. Commun.* 1896–1897. https://doi.org/10.1039/B304178F (2003).
12. Alleti, R., Perambuduru, M., Samantha, S. & Reddy, V. P. Gadolinium triflate: an efficient and convenient catalyst for acetylation of alcohols and amines. *J. Mol. Catal. Chem.* **226**, 57–59. https://doi.org/10.1016/j.molcata.2004.09.024 (2005).
13. Liu, Z., Ma, Q., Liu, Y. & Wang, Q. 4-(N, N-Dimethylamino) pyridine hydrochloride as a recyclable catalyst for acylation of inert alcohols: substrate scope and reaction mechanism. *Org. Lett.* **16**, 236–239. https://doi.org/10.1021/ol4030875 (2014).
14. Qi, S., Lan-Xiang, S., Ze-Mei, G., Tie-Ming, C. & Run-Tao, L. An efficient and green procedure for the Knoevenagel condensation catalyzed by Urea. *Chin. J. Chem.* **23**, 745–748. https://doi.org/10.1002/cjoc.200590745 (2005).
15. Devi, R., Begum, P., Bharali, P. & Deka, R. C. Comparative study of potassium salt-loaded MgAl hydrotalcites for the Knoevenagel condensation reaction. *ACS Omega*. **3**, 7086–7095. https://doi.org/10.1021/acsomega.8b00767 (2018).
16. Suresh & Sandhu, J. S. Recent advances in ionic liquids: green unconventional solvents of this century: part I. *Green. Chem. Lett. Rev.* **4**, 289–310. https://doi.org/10.1080/17518253.2011.572294 (2011).
17. Shokri, Z. & Zeynizadeh, B. Impregnated copper on Fe_3O_4: an efficient magnetically separable nanocatalyst for rapid and selective acylation of amines. *J. Iran. Chem. Soc.* **14**, 2467–2474. https://doi.org/10.1007/s13738-017-1181-2 (2017).
18. Kolagkis, P. X. et al. Deciphering the Knoevenagel condensation: towards a catalyst-free and water-mediated process. *Org. Biomol. Chem.* **22**, 8293–8299. https://doi.org/10.1039/D4OB01420K (2024).
19. Lim, C. W. & Lee, I. S. Magnetically recyclable nanocatalyst systems for the organic reactions. *Nano Today*. **5**, 412–434 (2010).
20. de Abrantes, P. G. et al. The efficient Knoevenagel condensation promoted by bifunctional heterogenized catalyst based chitosan-EDTA at room temperature. *Catal. Lett.* **153**, 945–955. https://doi.org/10.1007/s10562-022-04034-y (2023).
21. Dehghani, P., Elhamifar, D. & Kargar, S. Amine functionalized magnetic resorcinol formaldehyde as a green and reusable nanocatalyst for the Knoevenagel condensation. *Sci. Rep.* **15**, 2873. https://doi.org/10.1038/s41598-025-85921-3 (2025).
22. Zenebe, F. C., Taddesse, A. M., Sivasubramanian, M. & Babu, N. Highly efficient $CdS/CeO_2/Ag_3PO_4$ nanocomposite as novel heterogenous catalyst for Knoevenagel condensation and acetylation reactions. *Heliyon* https://doi.org/10.1016/j.heliyon.2024.e31798 (2024).
23. Somwanshi, S. B., Somvanshi, S. B. & Kharat, P. B. *J. Phys.:Conf. Ser.* 012046 (IOP Publishing).
24. Karimkhah, F., Elhamifar, D. & Shaker, M. Ag_2CO_3 containing magnetic nanocomposite as a powerful and recoverable catalyst for Knoevenagel condensation. *Sci. Rep.* **11**, 18736. https://doi.org/10.1038/s41598-021-98287-z (2021).
25. Makawana, A. Recent developments of metal and metal oxide nanocatalysts in organic synthesis. *Mini Rev. Med. Chem.* **16**, 1303–1320. https://doi.org/10.2174/1389557516666160823143243 (2016).
26. Chng, L. L., Erathodiyil, N. & Ying, J. Y. Nanostructured catalysts for organic transformations. *Acc. Chem. Res.* **46**, 1825–1837. https://doi.org/10.1021/ar300197s (2013).
27. Gawande, M. B., Pandey, R. K. & Jayaram, R. V. Role of mixed metal oxides in catalysis science—versatile applications in organic synthesis. *Catal. Sci. Technol.* **2**, 1113–1125. https://doi.org/10.1039/C2CY00490A (2012).
28. Gawande, M. B., Shelke, S. N., Zboril, R. & Varma, R. S. Microwave-assisted chemistry: synthetic applications for rapid assembly of nanomaterials and organics. *Acc. Chem. Res.* **47**, 1338–1348. https://doi.org/10.1021/ar400309b (2014).
29. Safaei-Ghomi, J., Shahbazi-Alavi, H. & Kalhor, S. CeO_2 nanoparticles: an efficient and robust catalyst for the synthesis of 2-amino-4, 6-diarylbenzene-1, 3-dicarbonitriles. *Monatsh Chem.* **147**, 1933–1937. https://doi.org/10.1007/s00706-016-1693-y (2016).
30. Kumar, B. V., Naik, H. S. B., Girija, D. & Kumar, B. V. ZnO nanoparticle as catalyst for efficient green one-pot synthesis of coumarins through Knoevenagel condensation. *J. Chem. Sci.* **123**, 615–621. https://doi.org/10.1007/s12039-011-0133-0 (2011).
31. Karimkhah, F., Elhamifar, D. & Shaker, M. Ag_2CO_3 containing magnetic nanocomposite as a powerful and recoverable catalyst for Knoevenagel condensation. *Sci. Rep.* **11**, 18736 (2021).
32. Shabalala, S., Maddila, S., van-Zyl, W. E. & Jonnalagadda, S. B. Sustainable CeO_2/ZrO_2 mixed oxide catalyst for the green synthesis of highly functionalized 1, 4-dihydropyridine-2, 3-dicarboxylate derivatives. *Curr. Org. Synth.* **15**, 396–403 (2018).
33. Sayed, M., Shi, Z., Gholami, F., Fatehi, P. & Soliman A. I. Ag@ TiO_2 nanocomposite as an efficient catalyst for Knoevenagel condensation. *ACS Omega*. **7**, 32393–32400 (2022).
34. Chen, X. et al. In situ pyrolysis of Ce-MOF to prepare CeO_2 catalyst with obviously improved catalytic performance for toluene combustion. *Chem. Eng. J.* **344**, 469–479. https://doi.org/10.1016/j.cej.2018.03.091 (2018).
35. Zheng, Y. et al. Facile synthesis and catalytic properties of CeO_2 with tunable morphologies from thermal transformation of cerium benzendicarboxylate complexes. *CrystEngComm* **13**, 1786–1788. https://doi.org/10.1039/C0CE00906G (2011).
36. Pirzada, B. M., Pushpendra, Kunchala, R. K. & Naidu, B. S. Synthesis of $LaFeO_3/Ag_2CO_3$ nanocomposites for photocatalytic degradation of Rhodamine B and p-chlorophenol under natural sunlight. *ACS Omega*. **4**, 2618–2629 (2019).
37. Taddesse, A. M., Bekele, T., Diaz, I. & Adgo, A. Polyaniline supported $CdS/CeO_2/Ag_3PO_4$ nanocomposite: an AB type tandem Nn heterojunctions with enhanced photocatalytic activity. *J. Photoch Photobio A*. **406**, 113005. https://doi.org/10.1016/j.jphotochem.2020.113005 (2021).
38. Wen, X. J. et al. Photocatalytic degradation of Levofloxacin by ternary Ag_2CO_3/CeO_2/AgBr photocatalyst under visible-light irradiation: degradation pathways, mineralization ability, and an accelerated interfacial charge transfer process study. *J. Catal.* **358**, 211–223. https://doi.org/10.1016/j.jcat.2017.12.005 (2018).
39. Ijaz, S., Ehsan, M. F., Ashiq, M. N., Karamat, N. & He, T. Preparation of $CdS@CeO_2$ core/shell composite for photocatalytic reduction of CO2 under visible-light irradiation. *Appl. Surf. Sci.* **390**, 550–559. https://doi.org/10.1016/j.apsusc.2016.08.098 (2016).
40. Farhadi, S., Jahanara, K. & Sepahdar, A. Sol–gel derived $LaFeO_3/SiO_2$ nanocomposite: synthesis, characterization and its application as a new, green and recoverable heterogeneous catalyst for the efficient acetylation of amines, alcohols and phenols. *J. Iran. Chem. Soc.* **11**, 1103–1112. https://doi.org/10.1007/s13738-013-0377-3 (2014).
41. Ningthoujam, R. et al. Nanocatalyst in remediating environmental pollutants. *Chem. Phys. Impact*. **4**, 100064. https://doi.org/10.1016/j.chphi.2022.100064 (2022).

42. Ijaz, S., Ehsan, M. F., Ashiq, M. N., Karamat, N. & He, T. J. A. S. S. Preparation of CdS@ CeO_2 core/shell composite for photocatalytic reduction of CO_2 under visible-light irradiation. **390**, 550–559 (2016).
43. Wu, C. Synthesis of Ag_2CO_3/CeO_2 microcomposite with visible light-driven photocatalytic activity. *Mater. Lett.* **152**, 76–78. https://doi.org/10.1016/j.matlet.2015.03.086 (2015).
44. Lin, A., Ibrahim, A. A., Arab, P., El-Kaderi, H. M. & El-Shall, M. S. Palladium nanoparticles supported on Ce-metal–organic framework for efficient CO oxidation and low-temperature CO_2 capture. *ACS Appl. Mater. Interfaces*. **9**, 17961–17968. https://doi.org/10.1021/acsami.7b03555 (2017).
45. Duan, W. et al. Fabrication of superhydrophobic cotton fabrics with UV protection based on CeO_2 particles. *Nd Eng. Chem. Res.* **50**, 4441–4445. https://doi.org/10.1021/ie101924v (2011).
46. Khalil, K. M., Elkabee, L. A. & Murphy, B. Preparation and characterization of thermally stable porous ceria aggregates formed via a sol–gel process of ultrasonically dispersed cerium (IV) isopropoxide. *Microporous Mesoporous Mater.* **78**, 83–89. https://doi.org/10.1016/j.micromeso.2004.09.019 (2005).
47. Postole, G. et al. Knoevenagel condensation reaction over acid–base bifunctional nanocrystalline $Ce_xZr_{1-x}O_2$ solid solutions. *J. Catal.* **269**, 110–121. https://doi.org/10.1016/j.jcat.2009.10.022 (2010).
48. Yu, X. et al. Preparation of hexagonal cerium oxide nanoflakes by a surfactant-free route and its optical property. *J. Mater. Res.* **22**, 3006–3013. https://doi.org/10.1557/JMR.2007.0408 (2007).
49. Ghazi, S., Rhouta, B., Tendero, C. & Maury, F. Synthesis, characterization and properties of sulfate-modified silver carbonate with enhanced visible light photocatalytic performance. *RSC Adv.* **13**, 23076–23086. https://doi.org/10.1039/D3RA03120A (2023).
50. Jia, J., Xu, Q., Fan, H., Lv, Y. & Li, D. Recent advances in catalytic asymmetric condensation reactions for the synthesis of nitrogen containing compounds. *Org. Chem. Front.* https://doi.org/10.1039/D4QO02078B (2025).
51. Dyson, P. J. & Jessop, P. G. Solvent effects in catalysis: rational improvements of catalysts via manipulation of solvent interactions. *Catal. Sci. Technol.* **6**, 3302–3316. https://doi.org/10.1039/C5CY02197A (2016).
52. Rathod, S., Navgire, M., Arbad, B. & Lande, M. Preparation of Mg-doped Ce-Zr solid catalysts and their catalytic potency for the synthesis of 5-arylidene-2, 4-thiazolidinediones via Knoevenagel condensation. *S Afr. J. Chem.* **65**, 196–201 (2012). http://journals.sabinet.co.za/sajchem/
53. Ezugwu, C. I. et al. An N-heterocyclic carbene based MOF catalyst for Sonogashira cross-coupling reaction. *Catal. Sci. Technol.* **6**, 2050–2054. https://doi.org/10.1039/C5CY01944C (2016).
54. Kalbasi, R. J. & Izadi, E. Synthesis and characterization of polymer/microporous molecular sieve nanocomposite as a shape-selective basic catalyst. *C R Chim.* **14**, 1002–1013. https://doi.org/10.1016/j.crci.2011.05.001 (2011).
55. Mukhopadhyay, C. & Datta, A. A simple, efficient and green procedure for the Knoevenagel condensation of aldehydes with N-methylpiperazine at room temperature under solvent-free conditions. *Synth. Commun.* **38**, 2103–2112. https://doi.org/10.1080/00397910802029364 (2008).
56. Jin, T. S., Zhang, J. S., Wang, A. Q. & Li, T. S. An efficient and environment friendly procedure for the synthesis of arylmethylenemalononitrile catalyzed by strong base anion-exchange resin in water. *Synth. Commun.* **34**, 2611–2616. https://doi.org/10.1081/SCC-200025621 (2004).
57. Carvalho, H. L. et al. A simple and efficient protocol for the Knoevenagel reaction of Benzylidenemalononitriles and the evaluation of the larvicidal activity on Aedes Aegypti. *Rev. Virtual Quim.* **10**, 362–374. https://doi.org/10.21577/1984-6835.20180028 (2018).
58. Santamarta, F., Verdia, P. & Tojo, E. A simple, efficient and green procedure for Knoevenagel reaction in [MMIm][MSO_4] ionic liquid. *Catal. Commun.* **9**, 1779–1781. https://doi.org/10.1016/j.catcom.2008.02.010 (2008).
59. Mobarakeh, M. I., Saffar-Teluri, A. & Tabrizi, S. H. Synthesis and characterization of Al_2O_3–SiO_2–MgO nanocomposite prepared by sol–gel process as an efficient catalyst for the Knoevenagel condensation of aldehydes with malononitrile. *Res. Chem. Intermed.* **41**, 6625–6633. https://doi.org/10.1007/s11164-014-1765-8 (2015).
60. Momayezan, M., Ghashang, M. & Hassanzadeh-Tabrizi, S. Barium aluminate nano-spheres grown on the surface of $BaAl_2O_4$: a versatile catalyst for the Knoevenagel condensation reaction of malononitrile with benzaldehyde. *Bulg. Chem. Commun.* **47**, 809–815 (2015).
61. Hosseini-Sarvari, M., Sharghi, H. & Etemad, S. Nanocrystalline ZnO for Knoevenagel condensation and reduction of the carbon, carbon double bond in conjugated alkenes. *Helv. Chim. Acta.* **91**, 715–724. https://doi.org/10.1002/hlca.200890072 (2008).
62. Schejn, A. et al. Fe_3O_4@ ZIF-8: magnetically recoverable catalysts by loading Fe_3O_4 nanoparticles inside a zinc imidazolate framework. *Dalton Trans.* **44**, 10136–10140. https://doi.org/10.1039/C5DT01191D (2015).
63. Burange, A. S., Tugaonkar, P. S., Thakur, S. D., Khan, R. R. & Shukla, R. Nano-crystalline $HoCrO_4$: efficient catalyst for Knoevenagel condensation in water: first catalytic application of cr (V) species. *Nano-Struct Nano-Objects*. **23**, 100493. https://doi.org/10.1016/j.nanoso.2020.100493 (2020).
64. Mishra, A., Yadav, P. & Awasthi, S. K. Nitrogen-Enriched Biguanidine-Functionalized Cobalt ferrite nanoparticles as a heterogeneous base catalyst for Knoevenagel condensation under Solvent-Free conditions. *ACS Org. Inorg. Au*. **3**, 254–265. https://doi.org/10.1021/acsorginorgau.3c00002 (2023).
65. Amić, A. & Molnar, M. An improved and efficient N-acetylation of amines using choline chloride based deep eutectic solvents. *Org. Prep Proced. Int.* **49**, 249–257. https://doi.org/10.1080/00304948.2017.1320914 (2017).
66. Roberts, C. W., Fanta, G. F. & Martin, J. D. Synthesis and spectra of a matched series of 1, 5-Disubstituted tetrazoles. *J. Org. Chem.* **24**, 654–657. https://doi.org/10.1021/jo01087a022 (1959).
67. Sodhi, R. K., Kumar, V. & Paul, S. M (acac) N covalently anchored onto amine functionalized silica: highly efficient and recyclable heterogeneous catalysts for the acetylation of amines, phenols and alcohols under solvent-free conditions. *Open. Catal. J.* **6** https://doi.org/10.2174/1876214X01306010001 (2013).
68. Aditya, D. Synthesis & characterization of 4-hydroxyacetanilide starting from acetanilide. *J. Med. Pharm. Allied Sci.* **73**, 73 (2016).
69. Saikia, U. P., Hussain, F. L., Suri, M. & Pahari, P. Selective N-acetylation of aromatic amines using acetonitrile as acylating agent. *Tetrahedron Lett.* **57**, 1158–1160. https://doi.org/10.1016/j.tetlet.2016.01.108 (2016).

Acknowledgements

The authors acknowledge to Haramaya University (HURG-2020-03-02-75, Ethiopia) and Dire Dawa University for their financial support. Additionally, JMY and AMT acknowledge the Spanish Research Council (CSIC) for funding provided through the COOPA20271, COOPB22002, and COOPB24072 projects.

Author contributions

G.A. S. Methodology, Investigation, Writing the first draft; A. M. T. Conceptualization, Methodology, Data-curation, Writing-Reviewing, Editing; N. B. Conceptualization, Methodology, Data-curation, Writing-Reviewing; and J. M. Y. Conceptualization, Methodology, Data-curation, Software, Formal analysis, Writing-Reviewing, Editing. All authors reviewed the manuscript.

Declarations

Competing interests
The authors declare no competing interests.

Additional information
Supplementary Information The online version contains supplementary material available at https://doi.org/10.1038/s41598-025-01567-1.

Correspondence and requests for materials should be addressed to J.M.Y.

Reprints and permissions information is available at www.nature.com/reprints.

Publisher's note Springer Nature remains neutral with regard to jurisdictional claims in published maps and institutional affiliations.

Open Access This article is licensed under a Creative Commons Attribution-NonCommercial-NoDerivatives 4.0 International License, which permits any non-commercial use, sharing, distribution and reproduction in any medium or format, as long as you give appropriate credit to the original author(s) and the source, provide a link to the Creative Commons licence, and indicate if you modified the licensed material. You do not have permission under this licence to share adapted material derived from this article or parts of it. The images or other third party material in this article are included in the article's Creative Commons licence, unless indicated otherwise in a credit line to the material. If material is not included in the article's Creative Commons licence and your intended use is not permitted by statutory regulation or exceeds the permitted use, you will need to obtain permission directly from the copyright holder. To view a copy of this licence, visit http://creativecommons.org/licenses/by-nc-nd/4.0/.

© The Author(s) 2025